

The Major Protein Arginine Methyltransferase in *Trypanosoma brucei* Functions as an Enzyme-Prozyme Complex*

Received for publication, September 5, 2016, and in revised form, December 14, 2016. Published, JBC Papers in Press, December 20, 2016, DOI 10.1074/jbc.M116.757112

Lucie Kafková[‡], Erik W. Debler[§], John C. Fisk[‡], Kanishk Jain[¶], Steven G. Clarke[¶], and Laurie K. Read^{¶1}

From the [‡]Department of Microbiology and Immunology, Witebsky Center for Microbial Pathogenesis and Immunology, and Jacobs School of Medicine and Biomedical Sciences, University at Buffalo, Buffalo, New York 14214, the [§]Laboratory of Cell Biology, The Rockefeller University, New York, New York 10065, and the [¶]Department of Chemistry and Biochemistry and The Molecular Biology Institute, UCLA, Los Angeles, California 90095

Edited by John M. Denu

Prozymes are catalytically inactive enzyme paralogs that dramatically stimulate the function of weakly active enzymes through complex formation. The two prozymes described to date reside in the polyamine biosynthesis pathway of the human parasite *Trypanosoma brucei*, an early branching eukaryote that lacks transcriptional regulation and regulates its proteome through posttranscriptional and posttranslational means. Arginine methylation is a common posttranslational modification in eukaryotes catalyzed by protein arginine methyltransferases (PRMTs) that are typically thought to function as homodimers. We demonstrate that a major *T. brucei* PRMT, *TbPRMT1*, functions as a heterotetrameric enzyme-prozyme pair. The inactive PRMT paralog, *TbPRMT1*^{PRO}, is essential for catalytic activity of the *TbPRMT1*^{ENZ} subunit. Mutational analysis definitively demonstrates that *TbPRMT1*^{ENZ} is the cofactor-binding subunit and carries all catalytic activity of the complex. Our results are the first demonstration of an obligate heteromeric PRMT, and they suggest that enzyme-prozyme organization is expanded in trypanosomes as a posttranslational means of enzyme regulation.

Trypanosoma brucei, the causative agent of human African trypanosomiasis, poses a severe health risk in Sub-Saharan Africa. An estimated 70 million people are at risk of the infection, and the World Health Organization estimates about 20,000 new cases per year (1). In the search for new treatments, understanding the basic biology of the parasite is a cornerstone on the path to discovery of novel biological processes that could potentially serve as drug targets (2). Despite the eukaryotic nature of *T. brucei*, the organism has been shown to harbor

many unique biological processes or, in some cases, to extensively utilize mechanisms that are rarely used in higher eukaryotes (3–5). The exceptional biology of trypanosomes is likely a consequence of their long separate evolutionary history and numerous adaptations to the parasitic lifestyle (6).

Trypanosomes undergo significant morphological and physiological changes during their life cycle, which includes transitions between mammalian and insect vector hosts that provide distinct environmental conditions and temperatures (7). Strikingly, these organisms accomplish adaptations to changing environments and differentiation to several distinct life cycle forms all in the absence of transcriptional control of their genome (3). Rather, gene expression is regulated at posttranscriptional and posttranslational levels. Posttranslational modification of proteins is one such mechanism that allows rapid responses to internal and external cues (8). Our proteome-wide studies revealed that about 15% of the proteome of *T. brucei* insect vector procyclic forms (PFs)² harbors arginine methyl marks (9, 10).³ Thus, arginine methylation is poised to play a crucial role in regulating *T. brucei* biology. In support of this notion, we showed that *TbPRMT1*-catalyzed arginine methylation of the essential RNA-binding protein DRBD18 acts as a switch that controls the RNA-stabilizing and -degrading activity of this major transcriptome regulator as well as the composition of DRBD18-containing ribonucleoproteins (11).

An enzyme family containing three major types of protein arginine methyltransferases (PRMTs) catalyzes arginine methylation (12). All PRMTs catalyze formation of ω -*N*^G-monomethylarginine (MMA), type I PRMTs catalyze ω -*N*^G,*N*^G-asymmetric dimethylarginine (ADMA), and type II PRMTs create ω -*N*^G,*N*^G-symmetric dimethylarginine (SDMA). Humans possess nine PRMTs (12). *T. brucei* apparently contains just four PRMTs, and we showed that together these enzymes have the capacity to catalyze MMA, ADMA, and SDMA formation (13–

* This work was supported by National Institutes of Health Grants R01 AI060260 (to L. K. R.) and R01 GM026020 (to S. G. C.), National Institutes of Health Ruth L. Kirschstein National Service Award GM007185 to (K. J.), and American Heart Association Predoctoral Fellowship 15PRE24480155 (to L. K.). The authors declare that they have no conflicts of interest with the contents of this article. The content is solely the responsibility of the authors and does not necessarily represent the official views of the National Institutes of Health.

¹ To whom correspondence should be addressed: Dept. of Microbiology and Immunology, University at Buffalo, Jacobs School of Medicine and Biomedical Sciences, Buffalo, NY 14214. Tel.: 716-829-3307; E-mail: lread@buffalo.edu.

² The abbreviations used are: PF, procyclic form; PRMT, protein arginine methyltransferase; *Tb*, *T. brucei*; MMA, ω -*N*^G-monomethylarginine; ADMA, ω -*N*^G,*N*^G-asymmetric dimethylarginine; SDMA, ω -*N*^G,*N*^G-symmetric dimethylarginine; BF, bloodstream form; LSH, linker-Strep-His; AdoMet, S-adenosyl-L-methionine; MBP, maltose-binding protein; MALS, multiangle light scattering; AdoMetDC, AdoMet decarboxylase; MCS, multiple cloning site; qRT-PCR, quantitative RT-PCR; qPCR, quantitative PCR.

³ K. Lott and L. Read, unpublished results.

T. brucei PRMT Is an Enzyme-Prozyme Pair

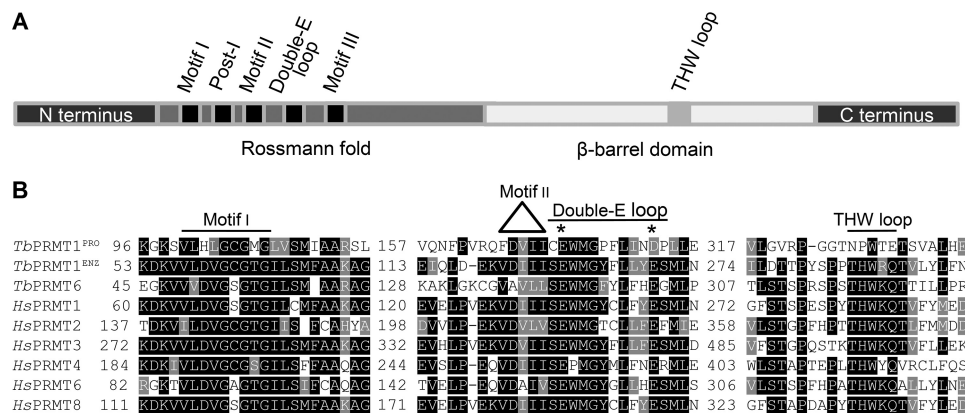


FIGURE 1. *TbPRMT1^{PRO}* lacks motifs important for PRMT activity. **A**, schematic representation of PRMT motifs (not to scale). **B**, selected motifs from Clustal Omega alignment of *T. brucei* and *Homo sapiens* type I PRMTs. * marks conserved residues in the double-E loop.

16). *TbPRMT7* was the first characterized PRMT to unquestionably create only MMA, making it a type III PRMT (13). *TbPRMT5*, despite its evolutionary divergence, exhibits a type II activity (15), and *TbPRMT6* and *TbPRMT1* have both been shown to create ADMA, therefore belonging to the type I PRMT group (14, 16). Like human PRMT1, *TbPRMT1* is responsible for the majority of ADMA formation *in vivo* (14, 17). However, perplexingly, *in vitro*, *TbPRMT1* exhibits a very narrow substrate specificity and weak activity (14). We recently showed that *TbPRMT1* protein stability is mutually dependent on a previously uncharacterized *T. brucei* PRMT paralog tentatively named *TbPRMT3* based on its homology to human PRMT3 (18). Typically, this type of mutual stability dependence is observed in proteins belonging to the same complex (19, 20). *TbPRMT3* has not exhibited any *in vitro* activity in our hands, and its primary sequence harbors mutations in conserved PRMT motifs; thus, we suspected it to be an inactive PRMT paralog. The observed *in vivo* dependence of a very weak enzyme and a catalytically dead paralog strikingly resembles a scenario that has been described in the *T. brucei* polyamine synthesis pathway: the prozyme paradigm (21). Here, the functional forms of two enzymes involved in polyamine biosynthesis consist of a barely active enzyme in complex with an inactive enzyme paralog, termed prozyme. The functional complex comprises two proteins in which the prozyme allosterically activates the enzyme, and the activity of the complex exceeds that of the “active” subunit alone on average by 2000-fold (19, 21).

In this study, we show that *TbPRMT1* functions as a heterotetrameric complex formed by the enzymatic subunit *TbPRMT1^{ENZ}* (previously *TbPRMT1*) and the inactive PRMT paralog *TbPRMT1^{PRO}* (previously *TbPRMT3*). Our results demonstrate a novel PRMT organization and represent the first expansion of the trypanosome prozyme paradigm outside the polyamine synthesis pathway. These findings suggest that allosteric enzyme activation by catalytically inactive paralogs may be a more widespread mechanism for posttranslational regulation in trypanosomes than previously appreciated. Furthermore, our results suggest the presence of novel PRMT regulatory mechanisms that could also function in higher organisms under specific conditions.

Results

TbPRMT1^{PRO} Is Missing Key Catalytic Residues—The *T. brucei* genome encodes five proteins with high homology to human PRMTs, four of which have been characterized previously (13–16). Pairwise BLAST comparisons with human PRMTs indicated that the remaining putative *TbPRMT* (*Tb927.10.3560*) has the highest sequence similarity to human PRMT3, and therefore this enzyme has been formerly referred to as *TbPRMT3* (18, 22). In light of the functional results presented in this work, we have renamed *Tb927.10.3560* as *TbPRMT1^{PRO}*. Our studies also have led us to rename the former *TbPRMT1* (*Tb927.1.4690*) as *TbPRMT1^{ENZ}*, and these names will be used hereafter. To begin to understand the function of *TbPRMT1^{PRO}*, we first examined its amino acid sequence. In general, type I PRMTs comprise a Rossmann fold that harbors conserved motifs I, post-I, II, and III and the double-E loop as well as a β -barrel domain containing a THW loop (Fig. 1A). The *TbPRMT1^{PRO}* amino acid sequence reveals conserved motifs I, post-I, II, and III. However, this protein harbors a Glu to Asp mutation within its double-E loop (Fig. 1B). Although conservative, the analogous mutation in rat PRMT1 was shown previously to decrease *in vitro* methylation activity to 0.03% compared with wild type enzyme (23). Furthermore, based on phylogenetic analysis, *TbPRMT1^{PRO}* clusters with type I PRMTs (24), and as such, it is expected to contain a THW loop. Strikingly, neither the threonine nor the histidine residue is conserved in the region of *TbPRMT1^{PRO}* corresponding to the THW loop (Fig. 1B). These observations suggested that *TbPRMT1^{PRO}* could be an inactive PRMT paralog.

TbPRMT1^{PRO} Forms a Complex with *TbPRMT1^{ENZ}*—*TbPRMT1^{ENZ}* has been described previously as an active enzyme that is responsible for the majority of ADMA formation *in vivo* (14). Surprisingly, *in vitro* we observed a narrow substrate specificity and very low activity compared with rat PRMT1 (14). Attempts to detect *TbPRMT1^{PRO}* activity have been unsuccessful, reinforcing the idea that it possibly is a catalytically inactive PRMT paralog. While investigating the interplay of *TbPRMTs* in *T. brucei* PF, we noticed that *TbPRMT1^{ENZ}* and *TbPRMT1^{PRO}* share mutual protein stability dependence (18). Because this phenomenon is commonly associated with proteins that form a complex, we explored the

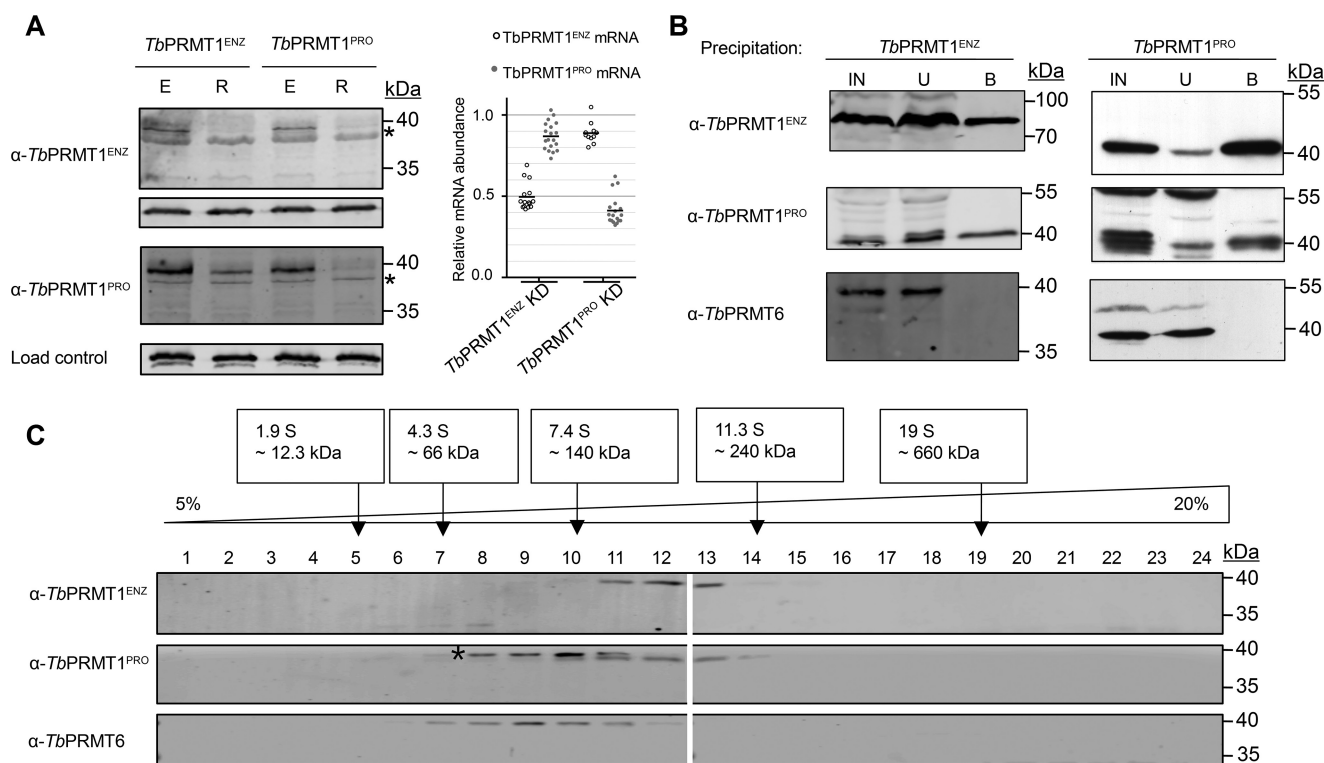


FIGURE 2. *TbPRMT1*^{ENZ} and *TbPRMT1*^{PRO} form a complex. *A, left*, the stabilities of *TbPRMT1*^{ENZ} and *TbPRMT1*^{PRO} proteins are mutually dependent. Lysed BF *T. brucei* cells with the indicated *TbPRMT* either expressed (E) or repressed (R) were probed with antibodies against specific *TbPRMTs*. α -p22 antibody was used as a load control. * marks a nonspecific band. The image is representative of three biological replicates. *A, right*, RNAi-mediated depletion of either *TbPRMT1*^{PRO} or *TbPRMT1*^{ENZ} mRNA does not significantly affect the mRNA level of their counterpart. mRNA levels of each *TbPRMT1* subunit were determined using qRT-PCR. Data were plotted as induced/uninduced RNAi cell mRNA levels. Data points represent technical replicates within two biological replicates. The horizontal line represents the mean. *B*, *TbPRMT1*^{ENZ}-Myc-BirA* and *TbPRMT1*^{PRO}-LSH were expressed from an exogenous locus in separate cell lines. Input (IN), unbound (U), and bound (B) proteins from precipitations of tagged *TbPRMTs* were probed with α -*TbPRMT* antibodies. α -*TbPRMT6* served as a specificity control. The image is representative of two biological replicates. *C*, glycerol gradient sedimentation patterns of *TbPRMT1*^{ENZ} and *TbPRMT1*^{PRO} overlap in a range suggesting a tetramer formation. Wild type 29-13 procyclic form *T. brucei* cell lysate was fractionated on a 5–20% glycerol gradient. Fractions were probed with α -*TbPRMT* antibodies. Size standards were run on a parallel gradient. * marks a contaminating species recognized by the *TbPRMT1*^{PRO} antibody. The image is representative of two biological replicates.

possibility that *TbPRMT1*^{ENZ} and *TbPRMT1*^{PRO} form a PRMT heteromeric complex. First, we asked whether the mutual stability dependence of *TbPRMT1*^{ENZ} and *TbPRMT1*^{PRO} is conserved in both culturable *T. brucei* life cycle stages. We induced RNAi of either *TbPRMT1*^{ENZ} or *TbPRMT1*^{PRO} in the clinically relevant bloodstream form (BF) *T. brucei* and used Western blotting to examine levels of both proteins (Fig. 2A, left). We observed a decrease in the protein levels of both proteins regardless of which PRMT was repressed. To rule out the possibility that our antibodies simply do not discriminate between *TbPRMT1*^{ENZ} and *TbPRMT1*^{PRO}, the antibodies were tested against *Escherichia coli*-expressed recombinant proteins. Fig. 3B, lanes a and c, clearly show the specificity of each antibody to its intended target. Furthermore, to ensure that our RNAi constructs were specific to only a single PRMT, we measured *TbPRMT1*^{ENZ} or *TbPRMT1*^{PRO} mRNA levels in both knock-down cell lines. In either case, we observed no significant change in the mRNA level of the non-target PRMT upon RNAi induction (Fig. 2A, right) as reported previously in the PF life cycle stage (18). Thus, the mutual stability dependence of *TbPRMT1*^{ENZ} and *TbPRMT1*^{PRO} occurs on the protein level in both life cycle stages.

Next, we investigated whether *TbPRMT1*^{ENZ} and *TbPRMT1*^{PRO} are a part of the same complex *in vivo*. Because the stability data

suggested the same mechanism in both life cycle stages, we performed all subsequent experiments in *T. brucei* PF, which grows to higher densities and therefore is more suitable for proteomic experiments. We expressed N-terminally tagged *TbPRMT1*^{ENZ}-Myc-BirA* and C-terminally tagged *TbPRMT1*^{PRO}-linker-Strep-His (LSH) in separate cell lines and precipitated the tagged proteins using α -Myc antibody or metal affinity resin, respectively. Western blots containing input, unbound, and bound samples were then probed with α -*TbPRMT1*^{ENZ}, α -*TbPRMT1*^{PRO}, and α -*TbPRMT6* antibodies (Fig. 2B). We observed that *TbPRMT1*^{ENZ} and *TbPRMT1*^{PRO} were efficiently precipitated in both reactions, whereas *TbPRMT6* was not present in either. These data are in agreement with our hypothesis that *TbPRMT1*^{ENZ} and *TbPRMT1*^{PRO} form a heteromer. To confirm this observation, we utilized a less direct but more native approach to investigate the same question. We lysed wild type PF *T. brucei* cells, separated native complexes on a 5–20% glycerol gradient, and probed the gradient fractions with α -*TbPRMT* antibodies (Fig. 2C). *TbPRMT1*^{ENZ} (39 kDa) and *TbPRMT1*^{PRO} (42 kDa) co-sedimented in fractions that, according to the size standards that were run on a parallel gradient, roughly correspond to a size of a tetramer (160 kDa). In multiple experiments, we noticed that α -*TbPRMT1*^{PRO} antibody detected two bands at ~40 kDa; however, upon

T. brucei PRMT Is an Enzyme-Prozyme Pair

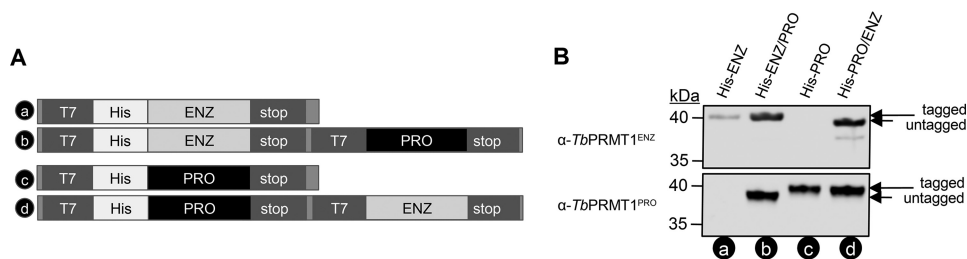


FIGURE 3. A, schematic of pETDuet-1 constructs used to express His-*TbPRMT1*^{ENZ} (a), His-*TbPRMT1*^{ENZ/PRO} (b), His-*TbPRMT1*^{PRO} (c), and His-*TbPRMT1*^{PRO/ENZ} (d). B, *TbPRMT1*^{ENZ} and *TbPRMT1*^{PRO} interact directly. Constructs a–d shown in A were expressed in *E. coli*. His-tagged protein was purified, and the elutions were probed with the indicated α -*TbPRMT* antibodies. The image is representative of two biological replicates.

induction of RNAi in PF cells, only the lower band was visibly diminished, leading us to conclude that the upper band is likely nonspecific (data not shown). In contrast to *TbPRMT1*^{ENZ} and *TbPRMT1*^{PRO}, *TbPRMT6* (41 kDa) peaked in a fraction corresponding to a dimer. Together, these data indicate that *TbPRMT1*^{ENZ} and *TbPRMT1*^{PRO} are part of the same complex *in vivo*.

As our *in vivo* studies did not allow us to determine whether *TbPRMT1*^{ENZ} and *TbPRMT1*^{PRO} interact directly, we used an *in vitro* approach to answer this question. To this end, we utilized a pETDuet bacterial expression vector that allows for co-expression of two proteins under separate T7 promoters (Fig. 3A). The two *TbPRMT1* subunits were first cloned separately to permit expression of a single histidine (His)-tagged PRMT (Fig. 3A, constructs “a” and “c”). For simplicity, these will be referred to as His-ENZ and His-PRO. In separate plasmids, the remaining *TbPRMT1* ORF was cloned into the second site, which resulted in two additional constructs containing His-*TbPRMT1*^{ENZ} with untagged *TbPRMT1*^{PRO} or His-*TbPRMT1*^{PRO} with untagged *TbPRMT1*^{ENZ}. These constructs will be hereafter referred to as His-ENZ/PRO and His-PRO/ENZ (Fig. 3A, constructs “b” and “d”). Each of the four constructs was separately expressed in *E. coli*, and metal affinity resin was used to purify the His-tagged protein under stringent washing conditions (1 M NaCl). Next, we probed Western blots containing the eluted proteins with α -*TbPRMT1*^{ENZ} and α -*TbPRMT1*^{PRO} antibodies (Fig. 3B). We observed that, in both cases, the untagged subunit was purified together with the His-tagged protein, clearly demonstrating a strong, direct non-ionic interaction between *TbPRMT1*^{ENZ} and *TbPRMT1*^{PRO}.

TbPRMT1^{ENZ}/*TbPRMT1*^{PRO} Heteromer Is the Functional Unit of the Major Type I PRMT in *T. brucei*—Having confirmed His-*TbPRMT1*^{ENZ}/*TbPRMT1*^{PRO} heteromer formation *in vivo* and *in vitro*, we next wanted to investigate the *in vitro* activity of the heteromer. Because our previous *TbPRMT1*^{ENZ} characterization showed that *TbPRMT1*^{ENZ} down-regulation almost completely abolishes ADMA formation in *T. brucei* (14), we expected the heteromer to exhibit activity comparable with the major mammalian type I PRMT, PRMT1. To test the PRMT activities of *TbPRMT1*^{ENZ}, *TbPRMT1*^{PRO}, and the heteromer containing both proteins and compare their activities with mammalian PRMT1, we incubated rat PRMT1, His-ENZ, His-PRO, His-ENZ/PRO, or His-PRO/ENZ with *S*-adenosyl-L-[methyl-³H]methionine ([³H]AdoMet) in the absence or presence of an RGG-rich substrate (Fig. 4). Following the reactions, proteins were resolved by SDS-PAGE and Coomassie-stained,

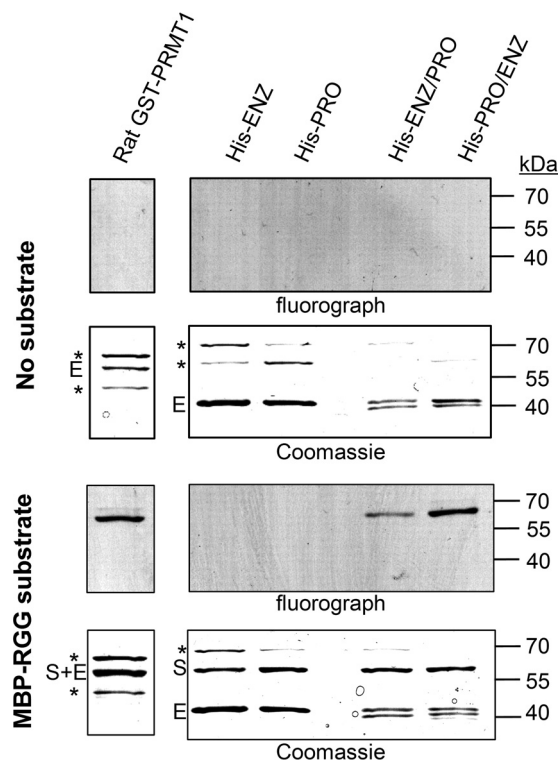


FIGURE 4. *TbPRMT1*^{ENZ/PRO} heteromer is the active form of a major *T. brucei* PRMT. For the *in vitro* methylation assay, MBP-RGG substrate was incubated with *TbPRMTs* in the presence of [³H]AdoMet. Proteins were separated by SDS-PAGE and visualized by fluorography and Coomassie staining. *TbPRMT1*^{ENZ} (His-ENZ) and *TbPRMT1*^{PRO} (His-PRO) do not exhibit any activity under the selected experimental conditions. The heteromer containing His-*TbPRMT1*^{PRO/ENZ} exhibits activity comparable with rat GST-PRMT1. Reactions where MBP-RGG was excluded were used as a control (no substrate). S, substrate; E, enzyme; *, contaminant. The image is representative of two technical replicates.

and the radiolabeled signal was visualized by fluorography. We observed that under our experimental conditions both heteromers, regardless of which subunit was fused to the N-terminal His tag, exhibited activity, whereas neither subunit alone produced any signal. Furthermore, the His-PRO/ENZ complex showed activity comparable with that of the rat PRMT1. From these data, we conclude that the *TbPRMT1*^{ENZ}/*TbPRMT1*^{PRO} heteromer is the active form of *TbPRMT1*.

We next wanted to determine the type of methylarginine produced by *TbPRMT1*. To this end, we performed a methylation reaction containing *TbPRMT1* heteromer, MBP-RGG substrate, and [³H]AdoMet. The reaction was allowed to proceed for 2 h based on a time course experiment showing that at this time point the reaction was progressing within the linear

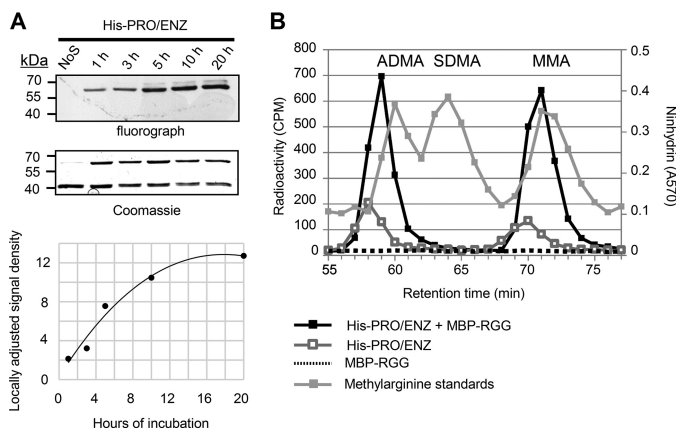


FIGURE 5. **A**, under our experimental conditions, His-PRO/ENZ complex activity progresses in a linear range at the 2-h reaction time. Five identical methylation reactions were set up. At each time point, a single reaction was quenched. After separation by SDS-PAGE, the gel was incubated with EN³HANCE solution for 1 h, dried, and exposed to film at -80 °C overnight. The density of each signal was measured and plotted (lower panel). NoS, no substrate was added to reaction. The image is representative of two technical replicates. **B**, high resolution ion exchange chromatography analysis of methylarginine derivatives catalyzed by His-*TbPRMT1*^{PRO/ENZ}. His-*TbPRMT1*^{PRO/ENZ} was incubated with substrate and TCA-precipitated. The resulting protein mixture was digested by acid hydrolysis. Amino acids were analyzed by cation exchange chromatography in the presence of unlabeled ADMA, SDMA, and MMA standards. The experiment was performed once.

range (Fig. 5A). Subsequently, the proteins were TCA-precipitated, hydrolyzed into amino acids, and analyzed on a cation exchange chromatography column together with unlabeled MMA, ADMA, and SDMA standards. Reactions omitting either substrate or enzyme served as controls (Fig. 5B). We observed a significant amount of ADMA and MMA present in the experimental sample, whereas no trace of SDMA was recorded. This led us to conclude that the *TbPRMT1* heteromer is a type I PRMT. We also observed a low level of both ADMA and MMA in the PRMT-only control. To determine whether this can be attributed to automethylation of the PRMT, we developed the gel presented in Fig. 4 for an additional month and concluded that the methylated species likely arise primarily from methylation of bacterial proteins that were present at low levels as contaminants in our *TbPRMT1* preparation (data not shown). Analysis of either *TbPRMT1*^{ENZ} or *TbPRMT1*^{PRO} alone by cation exchange chromatography revealed no activity as expected (data not shown), supporting the classification of *TbPRMT1*^{ENZ/TbPRMT1}^{PRO} heteromer as the major *T. brucei* type I PRMT.

***TbPRMT1* Forms a Heterotetramer in Solution**—Having determined that the *TbPRMT1* heteromer is a functional PRMT, we were intrigued by the possibility that this heteromer could be larger than the canonical PRMT dimer. The glycerol gradient sedimentation of native *TbPRMT1* complex suggested this enzyme could function as a tetramer (Fig. 2C). PRMTs can reportedly exist in large complexes *in vivo* (25, 26) and form homo-oligomers *in vitro* (27–30). Furthermore, the recent human PRMT8 crystal structure revealed a homotetrameric PRMT architecture, suggesting the possibility of heterotetrameric intermember interactions between two PRMT dimers (31). To investigate the size of the *TbPRMT1* heteromer we used multiangle light scattering (MALS). These studies showed that *TbPRMT1* adopts exclusively a tetrameric struc-

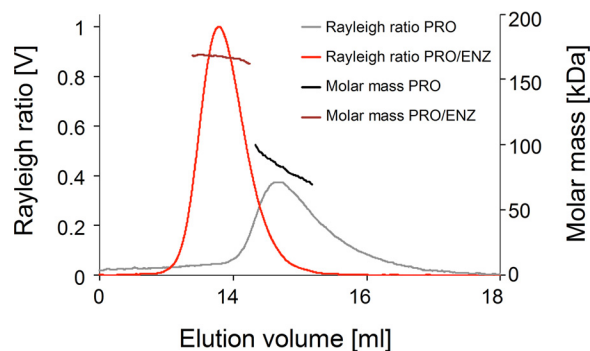


FIGURE 6. **Molecular mass determination and Rayleigh ratio of *TbPRMT1*^{ENZ/PRO} and of *TbPRMT1*^{PRO} by MALS coupled to size exclusion chromatography (Superdex 200 10/300 column).** The light scattering Rayleigh ratio (left ordinate; *TbPRMT1*^{ENZ/PRO}, light red; *TbPRMT1*^{PRO}, gray) and the molar mass distribution (right ordinate; *TbPRMT1*^{ENZ/PRO}, dark red; *TbPRMT1*^{PRO}, black) versus the elution volume are shown. *TbPRMT1*^{PRO} forms a heterotetramer, whereas *TbPRMT1*^{PRO} is dimeric. *TbPRMT1*^{ENZ} on its own is unstable and could therefore not be analyzed by MALS. The image is representative of two biological replicates.

ture (~160 kDa) in solution (Fig. 6). In contrast to the heteromer, *TbPRMT1*^{PRO} exists as a dimer in solution (Fig. 6). *TbPRMT1*^{ENZ} displays a high degree of aggregation when expressed alone, which precluded MALS analysis of this protein. Together, our data indicate that *TbPRMT1* requires both *TbPRMT1*^{ENZ} and *TbPRMT1*^{PRO} to adopt the active heterotetrameric structure.

***TbPRMT1*^{ENZ} Is the Catalytic Subunit of the *TbPRMT1* Heteromer**—The primary sequence of *TbPRMT1*^{PRO} suggested that it might be a catalytically inactive PRMT paralog. Furthermore, *TbPRMT1*^{ENZ}, despite its homology with human PRMT1, failed to show signs of catalytic activity in this study and only weak activity in our previous study (14). Together, these facts are reminiscent of a previously described prozyme paradigm typified by two different enzymes in the *T. brucei* polyamine biosynthesis pathway that function as heteromers in which an inactive enzyme paralog allosterically activates a catalytically active subunit (19, 21, 32, 33). With this paradigm and our data in mind, we asked whether *TbPRMT1*^{ENZ} is the sole subunit in the *TbPRMT1* complex that carries catalytic function. To investigate this possibility, we turned to a mutagenesis approach. We hypothesized that an introduction of mutations that are known to inactivate PRMTs into *TbPRMT1*^{ENZ} would lead to a total loss of heteromer activity, whereas the same mutations introduced into *TbPRMT1*^{PRO} sequence should leave the activity intact. Previous studies indicated that a mutation in conserved motif I residues leads to loss of PRMT activity, likely due to disruption of AdoMet binding (34, 35). Thus, we introduced a Gly to Arg mutation in the second Gly of the GXGXG in motif I of either *TbPRMT1*^{ENZ} or *TbPRMT1*^{PRO} in the context of the heteromeric enzyme. This mutation has been shown to completely abolish activity of a yeast PRMT1 homolog (35). To diversify our approach, we also introduced a mutation that would inactivate a PRMT by a different mechanism. We mutated the second Glu in the double-E loop to Gln (E135Q), a mutation previously shown to abolish PRMT activity without affecting AdoMet binding (23, 36). As noted above, *TbPRMT1*^{PRO} carries an Asp at this position (D180Q). Studies of mammalian PRMT1 showed that, although Glu to Asp muta-

T. brucei PRMT Is an Enzyme-Prozyme Pair

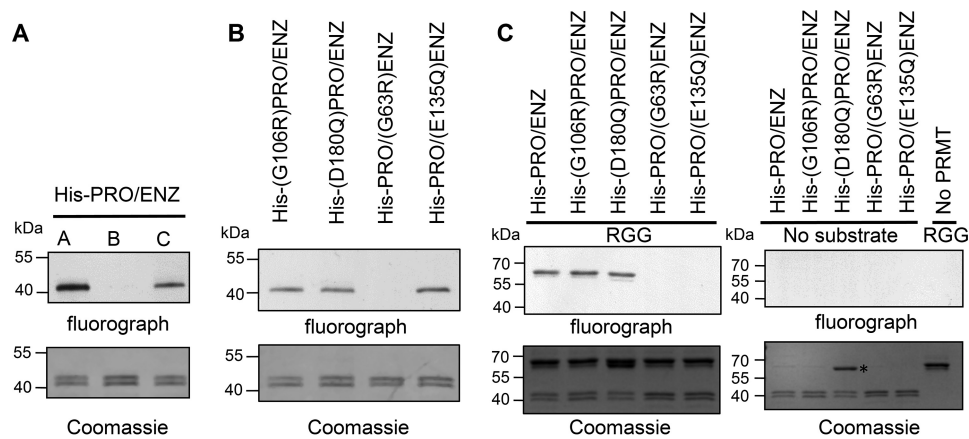


FIGURE 7. *TbPRMT1*^{ENZ} is the catalytic subunit of *TbPRMT1*^{ENZ/PRO} complex. *A*, AdoMet is specifically cross-linked to His-ENZ/PRO complex. His-ENZ/PRO was incubated with $[^3\text{H}]\text{AdoMet}$ (*A*). After 10 min of incubation, a 50-fold excess of unlabeled AdoMet (*B*) or dATP (*C*) was added. Samples were then incubated at 4 °C for ~18 h and UV cross-linked. After separation of proteins by SDS-PAGE, the gel was incubated with EN³HANCE solution for 1 h, dried, and exposed to film. The image is representative of two biological replicates. *B*, AdoMet binding capacity of *TbPRMT1*^{ENZ/PRO}. *TbPRMT1*s were incubated with $[^3\text{H}]\text{AdoMet}$ and UV cross-linked. Proteins were separated by SDS-PAGE and visualized by fluorography and Coomassie staining. Gly → Arg mutation targets AdoMet binding motif I, whereas Glu → Gln (or Asp → Gln in the case of *TbPRMT1*^{PRO}) emulates a mutation shown previously to abolish rat PRMT1 activity without affecting AdoMet binding capacity of the enzyme. The experiment was performed once. *C*, *in vitro* methylation assays of His-*TbPRMT1*^{PRO/ENZ} mutants. *TbPRMT1* wild type (His-PRO/ENZ) or mutant heteromers were incubated with MBP-RGG substrate in the presence of $[^3\text{H}]\text{AdoMet}$ (*left panel*). Proteins were separated by SDS-PAGE and visualized by fluorography and Coomassie staining. Either MBP-RGG substrate or PRMT was omitted in the control reactions (*right panel*). The image is representative of three technical replicates.

tion seriously hinders activity, Gln at this position completely abolished measurable PRMT activity (23).

The mutations described above were separately introduced into a pETDuet construct encoding for His-PRO and untagged ENZ (Fig. 3A, construct d), and the proteins were purified via the His tag. The presence of both proteins in these purifications was verified by Western blotting (data not shown), and the equimolar representation of each subunit was confirmed by visual examination of the Coomassie staining (Fig. 7).

First, we analyzed the AdoMet binding properties of wild type and mutant *TbPRMT1* heterotetramers to determine whether both subunits directly participate in AdoMet binding. Even in homodimeric yeast and mammalian PRMTs, it is not clear whether AdoMet binds to one or both monomers. Because deletion of the dimerization arm of rat PRMT1 leads to a complete loss of AdoMet binding, it is generally accepted that dimerization is a necessary prerequisite to bind AdoMet (23). Similarly, mutation of the dimerization arm was recently shown to abolish dimerization and catalytic activity in *TbPRMT7* (36). However, crystal structures of the conserved PRMT core show that the active site is likely formed within a single monomer rather than on the interface of the two subunits, leaving both subunits with equal potential to bind the cofactor (23, 36, 37). Interestingly, human PRMT8, which has been recently found to multimerize in solution, reportedly contains a single AdoMet molecule per dimer (31), although this finding has been challenged (38). In our case, despite the natural mutations in *TbPRMT1*^{PRO} that suggest inactivity, its motif I, which is thought to play an important role in AdoMet binding, is well conserved. Therefore, we could not rule out direct involvement of *TbPRMT1*^{PRO} subunit in AdoMet binding. To determine the roles of *TbPRMT1*^{ENZ} and *TbPRMT1*^{PRO} in AdoMet binding within the active heteromer, we UV cross-linked $[^3\text{H}]\text{AdoMet}$ to the His-PRO/ENZ heteromer, resolved the proteins by SDS-PAGE, and visualized the radioactive signal by fluorography.

We observed a single radioactive band whose signal was fully outcompeted by a 50-fold excess of unlabeled AdoMet but not by excess dATP, thereby demonstrating the specificity of the cross-linking (Fig. 7A). We then performed the same assay using the heteromers in which one of the subunits carried an inactivating mutation (Fig. 7B). We observed that both double-E loop mutants, His-(D180Q)PRO/ENZ and His-PRO/(E135Q)ENZ, were capable of AdoMet binding, which was in accord with mutational studies on mammalian PRMT1 showing that, although this residue in the double-E loop is crucial for catalysis, it contributes very little to AdoMet binding (23). The retained ability to bind AdoMet also reassured us that the introduced mutations do not distort protein folding. We next analyzed AdoMet binding in heteromers with motif I mutations in each of the subunits. Remarkably, although AdoMet binding of the heteromer was abolished when motif I of *TbPRMT1*^{ENZ} was mutated (Fig. 7B, His-PRO/(G63R)ENZ), the heteromer harboring mutation of motif I in the *TbPRMT1*^{PRO} subunit was perfectly capable of AdoMet binding (Fig. 7B, His-(G106R)PRO/ENZ). This led us to conclude that *TbPRMT1*^{ENZ} is the sole AdoMet-binding subunit of the complex.

To investigate the contribution of the *TbPRMT1*^{ENZ} and *TbPRMT1*^{PRO} subunits to the catalytic activity of the heteromeric *TbPRMT1* complex, we next performed a gel-based *in vitro* methylation assay. *TbPRMT1*, $[^3\text{H}]\text{AdoMet}$, and substrate were mixed and incubated for 18 h at 22 °C, and methylated products were visualized by fluorography (Fig. 7C). Heteromers containing mutations in either double-E loop (His-(D180Q)PRO/ENZ) or motif I (His-(G106R)PRO/ENZ) of *TbPRMT1*^{PRO} exhibited activity comparable with wild type complex. In stark contrast, complexes that carried mutations in either the double-E loop or motif I of *TbPRMT1*^{ENZ} were catalytically dead (Fig. 7C, His-PRO/(G63R)ENZ and His-PRO/(E135Q)ENZ). Therefore, we conclude that *TbPRMT1*^{ENZ} is the catalytic subunit of the *TbPRMT1* heterotetramer.

Discussion

In this report, we describe a novel mode of PRMT organization and function. *TbPRMT1*, the major type I PRMT in the early branching eukaryote *T. brucei* (14), is a functional heterotetramer comprising two subunits. The previously reported *TbPRMT1* protein (14, 22) (here renamed *TbPRMT1*^{ENZ}) bears a striking sequence identity to human PRMT1. By itself, *TbPRMT1*^{ENZ} exhibits no detectable activity under the conditions tested here despite retaining all critical PRMT motifs and displaying over 50% amino acid identity with human PRMT1. Nevertheless, *TbPRMT1*^{ENZ} constitutes the catalytically active subunit of the tetramer. The second subunit of the tetramer previously referred to as *TbPRMT3* (18, 22) is renamed here as *TbPRMT1*^{PRO}. *TbPRMT1*^{PRO} is catalytically inactive but is essential for the allosteric activation of *TbPRMT1*^{ENZ}. This unique PRMT organization represents the first reported obligate heteromeric PRMT in any organism.

Two other *T. brucei* enzymes, deoxyhypusine synthase and AdoMetDC, both within the polyamine synthesis pathway, have been shown to function in a similar manner (19, 21, 32, 33, 39). In both cases, a catalytically inactive enzyme paralog termed prozyme dramatically stimulates the function of the true enzyme. This mode of organization and activation was coined the “prozyme paradigm” by Phillips and co-workers (21), thus leading to the *TbPRMT1* naming convention described above. Inactive enzyme paralogs, called pseudoenzymes, are common in eukaryotes. By some estimates, 10% of human enzyme domains are predicted to be catalytically inactive, and this estimate is even higher for worms and flies at 15% (40). The importance of these proteins is becoming increasingly apparent as pseudoenzymes are assigned biological functions. For example, iRhoms, inactive enzymes resembling rhomboid proteases, act in the endoplasmic reticulum to promote degradation of specific proteins or maturation of others (41). In another example, ornithine decarboxylase homologs regulate activity of ornithine decarboxylases by countering their inhibitory antienzymes (42). Nevertheless, the degree of activation observed in trypanosome enzyme-prozyme pairs is exceptional. It has been postulated that the dramatic control of enzyme activities via the enzyme-prozyme mechanism was expanded in trypanosomes in response to their lack of transcriptional control and the almost exclusive reliance on posttranscriptional and posttranslational mechanisms of gene regulation (43). The present study is the first report of an enzyme-prozyme complex in trypanosomes outside the polyamine synthesis pathway. Our data suggest that this type of control mechanism may indeed be amplified in these organisms and that additional examples of enzyme-prozyme pairs likely await discovery in trypanosomes.

Novel means of enzyme regulation stemming from the enzyme-prozyme mechanism have been reported. For example, the AdoMetDC prozyme is present in limiting amounts, and it is rapidly up-regulated when AdoMetDC activity is chemically inhibited, allowing increased flux through the pathway (33). This regulation takes place at the level of prozyme translation, apparently triggered by decarboxylated AdoMet (44). *TbPRMT1* is unlikely to be controlled by an analogous

mechanism because the stabilities of *TbPRMT1*^{PRO} and *TbPRMT1*^{ENZ} proteins are mutually exclusive, similar to deoxyhypusine synthase and its prozyme (19). Intriguingly, however, *TbPRMT1*^{PRO}, but not *TbPRMT1*^{ENZ}, is reportedly phosphorylated (8, 45), bound to mRNA (46), and trafficked to stress granules in starved trypanosomes (47). This suggests that *TbPRMT1*^{PRO} could be, in certain situations, operating independently of *TbPRMT1*^{ENZ}, possibly as a homodimer (Fig. 6). An interesting observation made during our work was that, although *TbPRMT1*^{PRO} can be readily purified from *E. coli* in the absence of the enzyme, *TbPRMT1*^{ENZ} is notably unstable by itself and aggregates. This led us to postulate that *TbPRMT1*^{PRO} may act as a chaperone toward *TbPRMT1*^{ENZ}, and the mutual protein stability effect we observed could reflect different protein degradation mechanisms for the two subunits. In that case, sequestration of *TbPRMT1*^{PRO} into stress granules would efficiently abolish *TbPRMT1* activity for the duration of the stress and allow for a quick recovery once the cells enter a less hostile environment. Further research will focus on mechanisms of *TbPRMT1* regulation, allowing us to conclusively determine the advantages *T. brucei* gains from utilizing a heteromeric PRMT1.

The discovery of a heterotetrameric, prozyme-activated PRMT may also have relevance to methyltransferase organization and regulation in higher eukaryotes. The most striking parallel with the prozyme paradigm emerged from the work on the human RNA methyltransferase complex METTL3-METTL14. In this complex, METTL3 constitutes the catalytic core and binds AdoMet but requires allosteric activation and stabilization by METTL14 (48, 49). Although METTL14 has been reported to exhibit weak *in vitro* methylation activity (50), the phylogenetic analysis suggests that the METTL14 catalytic core has lost its function (51). In another example, mammalian PRMT7 and PRMT9 both harbor two catalytic modules in tandem, forming a pseudodimer. The data suggest that in both cases only the N-terminal PRMT module contains conserved residues and binds AdoMet, although the inactive module is necessary for the enzyme activity (52–55), which is somewhat reminiscent of activation of *TbPRMT1*^{ENZ} by *TbPRMT1*^{PRO}. In regard to possible PRMT multimerization, we show here that *TbPRMT1* forms a tetramer *in vitro* and sediments at a size corresponding to a tetramer in wild type cell lysate separated on a glycerol gradient. Based primarily on crystallographic studies, types I and III PRMTs are considered to function predominantly as homodimers with the exception of yeast PRMT1 (HMT1) (23, 27, 36, 37, 56, 57). However, two recent structural studies of human PRMT8 revealed a tetrameric enzyme bound to a single molecule of AdoMet per canonical dimer (31) or a possible octameric helical assembly (38). Furthermore, larger oligomers of type I PRMTs are often observed by both size exclusion chromatography and glycerol gradient fractionation, and some evidence suggests that the oligomerization may be necessary for PRMT activity (23, 28, 29, 38, 58, 59). Together, these findings imply that PRMT oligomerization may be more common than previously thought. Moreover, not only have PRMTs been shown to homo-oligomerize, but some studies support the possibility that PRMTs in mammals and plants have the ability to form heteromers. For example, mammalian PRMT2 can interact with PRMT1 both *in vivo* and *in vitro*,

T. brucei PRMT Is an Enzyme-Prozyme Pair

TABLE 1
List of primers

Primer name	Primer sequence
4A	AGTTC AATTGCTCGAGGGATCCATGTGGAGCC
4B	CCACATGGATCCCTCGAGCAATTGA
5A	ATCCGCAGTTCGAGAAGCATCATCACCATCA
5B	GGTGATGATGCTTCTCGAACTGCGGATGGCT
6A	CCACCATCACTTAGATAGA
6B	GATCTCTATCTAGAGTGATGGTGGTGAT
13A	TCCGAGGATCCGGTGGCTCCGGAGGTAGTA
13B	GATCTACTACCTCCGGAGCCACCGGATCCC
qPCR1 <i>TbPRMT1</i> ^{ENZ} 5'	CGTTCCTACTGCTTTGTTTG
qPCR1 <i>TbPRMT1</i> ^{ENZ} 3'	TTTCCGAGAAGTGGGAAGAG
qPCR1 <i>TbPRMT1</i> ^{PRO} 5'	GCGTGTATGGGGGTATTTAG
qPCR1 <i>TbPRMT1</i> ^{PRO} 3'	AACATGTTCTTGCACACGAC
qPCR2 <i>TbPRMT1</i> ^{ENZ} 5'	GGTTAAGGGCACAATTCGC
qPCR2 <i>TbPRMT1</i> ^{ENZ} 3'	ACACCTTTTGTTCCTCCGAG
qPCR2 <i>TbPRMT1</i> ^{PRO} 5'	GAAGCAATGTCTCACAGACT
qPCR2 <i>TbPRMT1</i> ^{PRO} 3'	AAGCAGACAAACAGACGCT
<i>TbPRMT1</i> ^{ENZ} 5' AflII	GACTTAAGATGACGGTGGACGCAAATGCCCGC
<i>TbPRMT1</i> ^{ENZ} BamHI 3' STOP	GAGGATCCCTACCGCAGCCGAAAAATCCTGG
BirA STOPdel 5'	CGCAGAGAAGCTCGAGCTTAAGATGACCGTG
BirA STOPdel 3'	CACCGTCATCTTAAGCTCGAGCTTCTCTGCG
pETDuet BamHI frame fix 5'	CATCATCACCAAGCCAGGATCCATG
pETDuet BamHI frame fix 3'	CATGGATCCTGCGCTGTGGTGATGATG
<i>TbPRMT1</i> ^{ENZ} -ORF-BamHI-5'	GTAGGATCCATGACCGTGGACGCAAAATG
<i>TbPRMT1</i> ^{ENZ} -ORF-HindIII-3'	GTAAGCTTCTACCGCAGCCGAAAAATCCT
<i>TbPRMT1</i> ^{ENZ} -ORF-NdeI-5'	GTACATATGATGACCGTGGACGCAAAATG
<i>TbPRMT1</i> ^{ENZ} -ORF-XhoI-3'	GTACTCGAGTACCGCAGCCGAAAAATCCT
<i>TbPRMT1</i> ^{PRO} -ORF-BamHI-5'	GTAGGATCCATGTCACCGAAGAAAACTCGG
<i>TbPRMT1</i> ^{PRO} ORF-HindIII-3'	GTAAGCTTTCAATACCTTTGGTAGTTGTACGTG
<i>TbPRMT1</i> ^{PRO} -ORF-NdeI-5'	GTACATATGATGTCACCGAAGAAAACTCGG
<i>TbPRMT1</i> ^{PRO} -ORF-XhoI-3'	GTACTCGAGTCAATACCTTTGGTAGTTGTACGTG
G63R <i>TbPRMT1</i> ^{ENZ} 5'	CTTGATGTTGGTTGCAGGACGGGAATCCTTTC
G63R <i>TbPRMT1</i> ^{ENZ} 3'	GAAGGATTCCTGCTGCAACCAACATCAAG
G106R <i>TbPRMT1</i> ^{PRO} 5'	GCATTTGGGGTGCAGAAATGGGGTTGG
G106R <i>TbPRMT1</i> ^{PRO} 3'	CCAACCCCATCTGCACCCCAAATGC
E135Q <i>TbPRMT1</i> ^{ENZ} 5'	TCCTACTCTATCAGTCTATGTTAAACACCG
E135Q <i>TbPRMT1</i> ^{ENZ} 3'	CGGTGTTTAAACATAGACTGATAGAGTAGGA
D180Q <i>TbPRMT1</i> ^{PRO} 5'	GACCATTCTTGATCAATCAGCCACTGCTAGAAGAGGC
D180Q <i>TbPRMT1</i> ^{PRO} 3'	GCCTCTCTTAGCAGTGGCTGATTGATCAAGAATGGTC

although the extent to which this occurs *in vivo* is unknown (60). Interestingly, recombinant PRMT2 enhanced the activity of recombinant PRMT1 up to 15-fold even when PRMT2 harbored inactivating mutations, suggesting a possible regulatory role for PRMT2. Human PRMT3 was first identified in a yeast two-hybrid screen using PRMT1 as bait (29), and the interaction of human PRMT1 and PRMT8 has been documented by several high throughput studies and directed experiments (61–64). In *Arabidopsis*, two CARM1 (PRMT4) homologs interact *in vitro* and *in vivo*, although homodimeric CARM1 complexes are also present (65). The functional significance of these heteromeric PRMT interactions remains to be explored. However, one possibility is that, although trypanosomes evolved to utilize heteromeric PRMT1 as their main arginine methylation enzyme, the same mechanism may be used in mammals and plants, albeit on a much smaller scale and under specific conditions, to provide an additional level of enzyme regulation.

Experimental Procedures

T. brucei Cell Culture and Generation of Cell Lines and Antibodies—*TbPRMT1*^{ENZ} and *TbPRMT1*^{PRO} doxycycline-inducible RNAi cell lines were generated as described (18). Briefly, plasmids were linearized using the NotI restriction site and electroporated into a BF single marker *T. brucei* strain (66) with the Amaxa Nucleofactor™ system. Cells were cultured in HMI-11 medium supplemented with 10% FBS (67). Transformants were selected with 2.5 μg/ml phleomycin, and clones

were obtained by limiting dilution. RNAi was induced for 4 days with 2.5 μg/ml doxycycline.

pLEW100-Myc-BirA* vector (68) was a kind gift from Graham Warren (Max F. Perutz Laboratories, University of Vienna and Medical University of Vienna, Vienna, Austria). The complete open reading frame for *TbPRMT1*^{ENZ} was amplified using *TbPRMT1*^{ENZ} 5' AflII and *TbPRMT1*^{ENZ} BamHI 3' STOP primers (primers listed in Table 1) and cloned into the AflII and BamHI sites of pLEW100-Myc-BirA*. To facilitate read-through of PRMT1 in these sites, the stop codon of Myc-BirA* was deleted using the primers BirA STOPdel 5' and BirA STOPdel 3'.

The plasmid pLEW100-LSH with a C-terminal linker followed by the Strep(II) tag and eight repeats of His was constructed as follows. First, Strep(II)-His₈ tag was cloned into pLEW100 (66) digested with HindIII/BamHI. 15 pmol of each primer used in the reaction described below was phosphorylated with T4 polynucleotide kinase (ThermoFisher) and ATP in manufacturer supplied buffer A for 30 min at 37 °C followed by inactivation for 10 min at 75 °C. Primer pairs were pooled and incubated at 94 °C for 1 min, 50 °C for 1 min, and 24 °C for 1 min to facilitate annealing. Primers 4A, 4B, 5A, 5B, 6A, and 6B were then pooled; the primer mixture (0.75 pmol of each primer) was ligated with 200 ng of restricted pLEW100 plasmid with T4 DNA ligase; and ligated plasmids were transformed into DH5-α *E. coli*. Linker was then added to the resulting plasmid by

digesting pLEW100-Strep(II)-His₈ with XhoI/BamHI and ligating in phosphorylated primers 13A and 13B as above. Both pLEW100-Myc-BirA*-PRMT1^{ENZ} and pLEW100-PRMT^{PRO}-LSH were linearized with NotI restriction enzyme and transfected into *T. brucei* strain 29-13 PF cells. Resultant cell lines were selected with 2.5 μg/ml phleomycin or 1 μg/ml puromycin, respectively. *TbPRMT1*^{ENZ}, *TbPRMT1*^{PRO}, *TbPRMT6*, and p22 antibodies were described previously (16, 18, 69).

Co-immunoprecipitation of PRMT1 Isoforms—The immunoprecipitation of *TbPRMT1*^{ENZ} with the tagged *TbPRMT1*^{PRO}-LSH was performed following a 4-day induction of *TbPRMT1*^{PRO}-LSH using 2.5 μg/ml tetracycline. Cells were pelleted and resuspended in 6.5 ml of PBS with 0.1% Nonidet P-40, an EDTA-free protease inhibitor tablet (Roche Applied Science; one tablet/50 ml of lysis buffer), 50 μg/ml DNase I, and 1 mM CaCl₂. Cells were lysed for 20 min at 4 °C followed by centrifugation at 14,400 × *g* for 15 min. The recovered supernatant was bound to TALON[®] cobalt beads (Clontech) for 1 h at 4 °C. The flow-through was collected followed by washing with 50 ml of PBS. Bound *TbPRMT1*^{PRO} was then eluted with 150 mM imidazole. Eluted fractions were analyzed by Western blotting.

The reciprocal immunoprecipitation was performed using PF cells expressing Myc-BirA*-PRMT1^{ENZ}. Cells were induced for 4 days using 2.5 μg/ml doxycycline and collected by centrifugation. The cell pellet was resuspended in 7.4 ml of PBS with 0.1% Nonidet P-40, an EDTA-free protease inhibitor tablet (one tablet/50 ml of lysis buffer), and 1 mM DTT. Cells were lysed for 20 min at 4 °C, and then the supernatant was collected by centrifugation at 14,400 × *g* for 15 min. The supernatant was then bound to 100 μl of anti-Myc-Sepharose beads (ICL, Inc.) for 3 h at 4 °C. The flow-through was collected, and the beads were rinsed with 20 ml of PBS with 0.1% Tween 20. Bound *TbPRMT1*^{ENZ} was eluted with 100 mM glycine (pH 2.5) directly into 1 M Tris (pH 8.7) to neutralize the elutions. Eluted fractions were analyzed by Western blotting.

Recombinant Protein Cloning, Mutagenesis, and Expression—*TbPRMT1* was expressed in BL21 *E. coli* strain using pETDuet-1 vector that allows for co-expression of two genes under separate T7 promoters. First, we inserted a single nucleotide into pETDuet-1 sequence between the His tag and BamHI site to correct a frameshift that would arise from using said site (primers pETDuet BamHI frame fix 5' and pETDuet BamHI frame fix 3'). The *TbPRMT1*^{ENZ} or *TbPRMT1*^{PRO} full open reading frame, excluding the stop codon, was then amplified using *TbPRMT1*^{ENZ}-ORF-BamHI-5' and *TbPRMT1*^{ENZ}-ORF-HindIII-3' or *TbPRMT1*^{PRO}-ORF-BamHI-5' and *TbPRMT1*^{PRO}-ORF-HindIII-3' primers and cloned into the first multiple cloning site (MCS) using BamHI/HindIII restriction sites (Fig. 3A, constructs a and c) to allow for expression of a single N-terminally His-tagged protein. To generate constructs b and d (Fig. 3A), the full open reading frame of the second *TbPRMT1* subunit, including the stop codon, was amplified with *TbPRMT1*^{ENZ}-ORF-NdeI-5' and *TbPRMT1*^{ENZ}-ORF-XhoI-3' or *TbPRMT1*^{PRO}-ORF-NdeI-5' and *TbPRMT1*^{PRO}-ORF-XhoI-3' primers and cloned into the NdeI/XhoI site. Construct d was then used to generate catalytically inactive mutants. Overlapping primers containing the desired mutation were extended by KOD Hot

Start DNA polymerase (Novagen) and digested overnight by DpnI prior to transformation.

Recombinant protein expression was induced in BL21 *E. coli* strain by adding 0.1 mM isopropyl 1-thio-β-D-galactopyranoside and subsequent growth at 18 °C overnight. Bacterial pellets were resuspended and incubated for 20 min in PBS (pH 7.4) supplemented with 0.1 mM PMSF, 50 μg/ml DNase I (Sigma), 1 mM CaCl₂, and 50 μg/ml lysozyme and then sonicated. NaCl was then added at 1 M followed by three more rounds of sonication. The lysate was centrifuged for 20 min at 25,000 × *g*, and the supernatant was incubated for 3.5 h with TALON metal affinity resin (Clontech). The resin was washed, and proteins were eluted with PBS containing 200 mM imidazole. Samples were then dialyzed against PBS and flash frozen. The purification protocol of mutant protein included 10 μg/ml RNase A during lysis and 15 mM imidazole throughout. Rat GST-PRMT1 and MBP-RGG substrate were expressed and purified as described previously (14, 70).

The protein used for light scattering was expressed from a pETDuet-1 vector with *TbPRMT1*^{PRO} in MCS1 (restriction sites NcoI and NotI) and *TbPRMT1*^{ENZ} in MCS2 (NdeI and XhoI). The vector contained a PreScission protease (GE Healthcare) cleavage site for His tag removal from *TbPRMT1*^{PRO}. Protein expression followed the same protocol as described previously for *TbPRMT7* (36). Briefly, protein purification encompassed affinity chromatography on a nickel-nitrilotriacetic acid column (Qiagen), ion exchange chromatography on a HiTrap Heparin HP 5-ml column (GE Healthcare), and gel filtration on a HiLoad Superdex 200 16/60 column (GE Healthcare).

In Vitro Methylation Assays and Methylated Species Identification—*In vitro* methylation assays were performed as described previously (14). Briefly, 1.2 μM total PRMT was mixed with 0.2 or 2 μM substrate and 0.7 μM [³H]AdoMet (55–85 Ci (2.03–3.15 TBq)/mmol; PerkinElmer Life Sciences) in PBS (pH 7.4) containing 1 mM PMSF in a final volume of 50 μl. Reactions were carried out for ~18 h at 22 °C. After separation by SDS-PAGE, the gel was incubated with EN³HANCE solution (PerkinElmer Life Sciences) for 1 h, dried, and exposed to film at –80 °C overnight. The samples shown in Fig. 7C also contained 2 mM DTT, which led to substantial reduction of necessary exposure time from ~18 to 1 h.

Time Course of His-PRO/ENZ Complex Activity—Under our experimental conditions, we showed that product formation from the His-PRO/ENZ complex was linearly dependent upon time for at least the 2-hour reaction time used for chromatographic analysis in Fig. 5B. Five PBS-based reactions containing 60 pmol of His-PRO/ENZ, 10 pmol of MBP-RGG substrate, and 1 mM PMSF were initiated by addition of 2 μCi of [³H]-AdoMet (55–85 Ci (2.03–3.15 TBq)/mmol). The total reaction volume was 50 μl. *In vitro* methylation was allowed to progress for 1, 3, 5, 10, and 20 h; reactions were stopped by the addition of SDS sample buffer. After separation by SDS-PAGE, the gel was incubated with EN³HANCE solution for 1 h, dried, and exposed to film at –80 °C overnight.

Identification of methylarginine species was performed as described previously (36). Briefly, His-*TbPRMT1*^{PRO/ENZ} was incubated with substrate and TCA-precipitated. The resulting protein mixture was digested by acid hydrolysis. Amino acids

T. brucei PRMT Is an Enzyme-Prozyme Pair

were analyzed by cation exchange chromatography in the presence of unlabeled ADMA, SDMA, and MMA standards.

AdoMet-PRMT UV Cross-linking—To cross-link PRMTs to [³H]AdoMet, 1.6 μM total PRMT was mixed with 1.4 μM [³H]-AdoMet (78 Ci/mmol) in 50 mM phosphate buffer (pH 7.4) in the presence of 5 mM DTT in a final volume of 50 μl and incubated at 4 °C for ~18 h. Samples were then UV cross-linked for 10 min on ice 1 cm from the UV lamp using a UV Stratalinker 2400 (Stratagene). After separation of proteins by SDS-PAGE, the gel was Coomassie-stained, incubated with EN³HANCE solution for 1 h, dried, and exposed to film at –80 °C for 1 week.

To determine the specificity of UV cross-linking assay to AdoMet, 1.6 μM total PRMT was mixed with 1.4 μM [³H]-AdoMet in 50 mM phosphate buffer (pH 7.4) in the presence of 5 mM DTT and incubated at 22 °C for ~10 min (50-μl reaction volume). Following initial incubation, a 50× excess of dATP or unlabeled AdoMet was added to control reactions. Samples were then incubated at 4 °C for ~18 h. Samples were UV cross-linked for 10 min on ice 1 cm from the UV lamp using a UV Stratalinker 2400. After separation of proteins by SDS-PAGE, the gel was Coomassie-stained, incubated with EN³HANCE solution for 1 h, dried, and exposed to film at –80 °C for 1 week.

Multiangle Light Scattering—Untagged *Tb*PRMT1^{ENZ/PRO} and *Tb*PRMT1^{PRO} were characterized by multiangle light scattering following size exclusion chromatography. The identity of the proteins used for light scattering analysis was confirmed by mass spectrometry analysis. Protein at 50 μM (*Tb*PRMT1^{ENZ/PRO}) and 130 μM (*Tb*PRMT1^{PRO}) was injected onto a Superdex 200 10/300 GL size exclusion chromatography column equilibrated in a buffer containing 20 mM HEPES (pH 7.5), 200 mM NaCl, and 0.5 mM tris(2-carboxyethyl)phosphine. The chromatography system was connected in series with an 18-angle light scattering detector (DAWN HELEOS) and refractive index detector (OptilabrEX) (Wyatt Technology). Data were collected every second at a flow rate of 0.15 ml/min at 25 °C. Data analysis was carried out using the program ASTRA, yielding the molar mass and mass distribution (polydispersity) of the sample.

Quantitative RT-PCR—*Tb*PRMT1^{ENZ} and *Tb*PRMT1^{PRO} RNAi cell lines were grown for 4 days in the absence or presence of 2.5 (replicate 1) or 4 μg/ml (replicate 2) doxycycline. 250 ml of each cell culture was then harvested and resuspended in 1 ml of TRIzol reagent (Ambion). RNA was isolated according to the manufacturer's instructions and subsequently re-extracted by an acidic phenol RNA purification procedure. 10 μg of RNA/sample was DNase-treated using an Ambion DNA-free kit (Invitrogen) and re-extracted with acidic phenol. cDNA was synthesized using random hexamer primers with an iScript Select cDNA Synthesis kit (Bio-Rad) according to the manufacturer's instructions. Levels of each PRMT mRNA were then assayed by qRT-PCR using qPCR1 *Tb*PRMT1^{ENZ} and qPCR1 *Tb*PRMT1^{PRO} primer pairs in the first replicate. Second replicate qPCR used primer pairs qPCR2 *Tb*PRMT1^{ENZ} and qPCR2 *Tb*PRMT1^{PRO}. Between samples, mRNA levels were normalized to the levels of β-tubulin mRNA.

Glycerol Gradient Sedimentation—5–20% glycerol gradients were prepared as follows. 5.5 ml of buffer A (20 mM HEPES (pH 7.9), 10 mM MgCl₂, 50 mM KCl, 1 mM EDTA, and 20% glycerol) was poured into an ultracentrifugation tube and frozen at

–80 °C. 5.5 ml of buffer B (20 mM HEPES (pH 7.9), 10 mM MgCl₂, 50 mM KCl, 1 mM EDTA, and 5% glycerol) was layered on top of the frozen buffer A. The tubes then underwent four freeze/thaw cycles at –80 °C to create a linear glycerol gradient. 1 × 10⁹ wild type 29-13 procyclic form *T. brucei* cells per sample were harvested. The cell pellet was resuspended in 0.5 ml of lysis buffer (10 mM Tris (pH 8.0), 150 mM NaCl, 0.1% Nonidet P-40, an EDTA-free protease inhibitor tablet (one tablet/50 ml of lysis buffer), 50 μg/ml DNase I, and 1 mM CaCl₂). Cells were lysed for 20 min at 4 °C by addition of Triton X-100 to a final concentration of 1% (v/v). Lysates were cleared by centrifugation for 15 min at 15,000 × *g*. Cleared lysate was loaded on top of a 5–20% gradient and centrifuged at 32,000 rpm for 16 h in an SW41 Beckman rotor. Size standards consisting of proteins with known sedimentation coefficients were run on a parallel gradient (cytochrome *c* (1.9S), BSA (4.3S), yeast alcohol dehydrogenase (7.4S), catalase (11.3S), and thyroglobulin (19S)). 0.5-ml fractions were collected and probed with α-*Tb*PRMT antibodies. Size standard fraction contents were visualized by Coomassie staining.

Author Contributions—L. K. R., L. K., S. G. C., and E. W. D. conceived the project. L. K., E. W. D., J. C. F., and K. J. carried out the experiments. All authors contributed to interpretation of the data. L. K. and L. K. R. wrote the manuscript, and S. G. C. and E. W. D. provided valuable support with the writing.

Acknowledgments—We thank Kyle Smith (University at Buffalo) and Doris Berman (Rockefeller University) for technical assistance, Günter Blobel (Rockefeller University) for support, and David King (University of California, Berkeley) for mass spectrometry analysis.

References

1. Keating, J., Yukich, J. O., Sutherland, C. S., Woods, G., and Tediosi, F. (2015) Human African trypanosomiasis prevention, treatment and control costs: a systematic review. *Acta Trop.* **150**, 4–13
2. Bilbe, G. (2015) Infectious diseases. Overcoming neglect of kinetoplastid diseases. *Science* **348**, 974–976
3. Daniels, J. P., Gull, K., and Wickstead, B. (2010) Cell biology of the trypanosome genome. *Microbiol. Mol. Biol. Rev.* **74**, 552–569
4. Ferguson, M. A. (1999) The structure, biosynthesis and functions of glycosylphosphatidylinositol anchors, and the contributions of trypanosome research. *J. Cell Sci.* **112**, 2799–2809
5. Read, L. K., Lukeš, J., and Hashimi, H. (2016) Trypanosome RNA editing: the complexity of getting U in and taking U out. *Wiley Interdiscip. Rev. RNA* **7**, 33–51
6. Cavalier-Smith, T. (2010) Kingdoms Protozoa and Chromista and the eozoan root of the eukaryotic tree. *Biol. Lett.* **6**, 342–345
7. Vickerman, K. (1985) Developmental cycles and biology of pathogenic trypanosomes. *Br. Med. Bull.* **41**, 105–114
8. Urbaniak, M. D., Martin, D. M., and Ferguson, M. A. (2013) Global quantitative SILAC phosphoproteomics reveals differential phosphorylation is widespread between the procyclic and bloodstream form lifecycle stages of *Trypanosoma brucei*. *J. Proteome Res.* **12**, 2233–2244
9. Lott, K., Li, J., Fisk, J. C., Wang, H., Aletta, J. M., Qu, J., and Read, L. K. (2013) Global proteomic analysis in trypanosomes reveals unique proteins and conserved cellular processes impacted by arginine methylation. *J. Proteomics* **91**, 210–225
10. Fisk, J. C., Li, J., Wang, H., Aletta, J. M., Qu, J., and Read, L. K. (2013) Proteomic analysis reveals diverse classes of arginine methylproteins in mitochondria of trypanosomes. *Mol. Cell. Proteomics* **12**, 302–311

11. Lott, K., Mukhopadhyay, S., Li, J., Wang, J., Yao, J., Sun, Y., Qu, J., and Read, L. K. (2015) Arginine methylation of DRBD18 differentially impacts its opposing effects on the trypanosome transcriptome. *Nucleic Acids Res.* **43**, 5501–5523
12. Bedford, M. T., and Clarke, S. G. (2009) Protein arginine methylation in mammals: who, what, and why. *Mol. Cell* **33**, 1–13
13. Fisk, J. C., Sayegh, J., Zurita-Lopez, C., Menon, S., Presnyak, V., Clarke, S. G., and Read, L. K. (2009) A type III protein arginine methyltransferase from the protozoan parasite *Trypanosoma brucei*. *J. Biol. Chem.* **284**, 11590–11600
14. Pelletier, M., Pasternack, D. A., and Read, L. K. (2005) *In vitro* and *in vivo* analysis of the major type I protein arginine methyltransferase from *Trypanosoma brucei*. *Mol. Biochem. Parasitol.* **144**, 206–217
15. Pasternack, D. A., Sayegh, J., Clarke, S., and Read, L. K. (2007) Evolutionarily divergent type II protein arginine methyltransferase in *Trypanosoma brucei*. *Eukaryot. Cell* **6**, 1665–1681
16. Fisk, J. C., Zurita-Lopez, C., Sayegh, J., Tomasello, D. L., Clarke, S. G., and Read, L. K. (2010) TbPRMT6 is a type I protein arginine methyltransferase that contributes to cytokinesis in *Trypanosoma brucei*. *Eukaryot. Cell* **9**, 866–877
17. Tang, J., Frankel, A., Cook, R. J., Kim, S., Paik, W. K., Williams, K. R., Clarke, S., and Herschman, H. R. (2000) PRMT1 is the predominant type I protein arginine methyltransferase in mammalian cells. *J. Biol. Chem.* **275**, 7723–7730
18. Lott, K., Zhu, L., Fisk, J. C., Tomasello, D. L., and Read, L. K. (2014) Functional interplay between protein arginine methyltransferases in *Trypanosoma brucei*. *Microbiol. Open* **3**, 595–609
19. Nguyen, S., Jones, D. C., Wyllie, S., Fairlamb, A. H., and Phillips, M. A. (2013) Allosteric activation of trypanosomatid deoxyhypusine synthase by a catalytically dead paralog. *J. Biol. Chem.* **288**, 15256–15267
20. Hashimi, H., Cicová, Z., Novotná, L., Wen, Y. Z., and Lukes, J. (2009) Kinetoplastid guide RNA biogenesis is dependent on subunits of the mitochondrial RNA binding complex 1 and mitochondrial RNA polymerase. *RNA* **15**, 588–599
21. Willert, E. K., Fitzpatrick, R., and Phillips, M. A. (2007) Allosteric regulation of an essential trypanosome polyamine biosynthetic enzyme by a catalytically dead homolog. *Proc. Natl. Acad. Sci. U.S.A.* **104**, 8275–8280
22. Fisk, J. C., and Read, L. K. (2011) Protein arginine methylation in parasitic protozoa. *Eukaryot. Cell* **10**, 1013–1022
23. Zhang, X., and Cheng, X. (2003) Structure of the predominant protein arginine methyltransferase PRMT1 and analysis of its binding to substrate peptides. *Structure* **11**, 509–520
24. Wang, Y. C., Wang, J. D., Chen, C. H., Chen, Y. W., and Li, C. (2015) A novel BLAST-based relative distance (BBRD) method can effectively group members of protein arginine methyltransferases and suggest their evolutionary relationship. *Mol. Phylogenet. Evol.* **84**, 101–111
25. Gary, J. D., and Clarke, S. (1998) RNA and protein interactions modulated by protein arginine methylation. *Prog. Nucleic Acid. Res. Mol. Biol.* **61**, 65–131
26. Hung, C. J., Chen, D. H., Shen, Y. T., Li, Y. C., Lin, Y. W., Hsieh, M., and Li, C. (2007) Characterization of protein arginine methyltransferases in porcine brain. *J. Biochem. Mol. Biol.* **40**, 617–624
27. Troffer-Charlier, N., Cura, V., Hassenboehler, P., Moras, D., and Cavarelli, J. (2007) Functional insights from structures of coactivator-associated arginine methyltransferase 1 domains. *EMBO J.* **26**, 4391–4401
28. Lin, W. J., Gary, J. D., Yang, M. C., Clarke, S., and Herschman, H. R. (1996) The mammalian immediate-early TIS21 protein and the leukemia-associated BTG1 protein interact with a protein-arginine N-methyltransferase. *J. Biol. Chem.* **271**, 15034–15044
29. Tang, J., Gary, J. D., Clarke, S., and Herschman, H. R. (1998) PRMT 3, a type I protein arginine N-methyltransferase that differs from PRMT1 in its oligomerization, subcellular localization, substrate specificity, and regulation. *J. Biol. Chem.* **273**, 16935–16945
30. Rho, J., Choi, S., Seong, Y. R., Cho, W. K., Kim, S. H., and Im, D. S. (2001) Prmt5, which forms distinct homo-oligomers, is a member of the protein-arginine methyltransferase family. *J. Biol. Chem.* **276**, 11393–11401
31. Lee, W. C., Lin, W. L., Matsui, T., Chen, E. S., Wei, T. Y., Lin, W. H., Hu, H., Zheng, Y. G., Tsai, M. D., and Ho, M. C. (2015) Protein arginine methyltransferase 8: tetrameric structure and protein substrate specificity. *Biochemistry* **54**, 7514–7523
32. Velez, N., Brautigam, C. A., and Phillips, M. A. (2013) *Trypanosoma brucei* S-adenosylmethionine decarboxylase N terminus is essential for allosteric activation by the regulatory subunit prozyme. *J. Biol. Chem.* **288**, 5232–5240
33. Willert, E. K., and Phillips, M. A. (2008) Regulated expression of an essential allosteric activator of polyamine biosynthesis in African trypanosomes. *PLoS Pathog.* **4**, e1000183
34. Neault, M., Mallette, F. A., Vogel, G., Michaud-Levesque, J., and Richard, S. (2012) Ablation of PRMT6 reveals a role as a negative transcriptional regulator of the p53 tumor suppressor. *Nucleic Acids Res.* **40**, 9513–9521
35. McBride, A. E., Weiss, V. H., Kim, H. K., Hogle, J. M., and Silver, P. A. (2000) Analysis of the yeast arginine methyltransferase Hmt1p/Rmt1p and its *in vivo* function. Cofactor binding and substrate interactions. *J. Biol. Chem.* **275**, 3128–3136
36. Debler, E. W., Jain, K., Warmack, R. A., Feng, Y., Clarke, S. G., Blobel, G., and Stavropoulos, P. (2016) A glutamate/aspartate switch controls product specificity in a protein arginine methyltransferase. *Proc. Natl. Acad. Sci. U.S.A.* **113**, 2068–2073
37. Zhang, X., Zhou, L., and Cheng, X. (2000) Crystal structure of the conserved core of protein arginine methyltransferase PRMT3. *EMBO J.* **19**, 3509–3519
38. Toma-Fukai, S., Kim, J. D., Park, K. E., Kuwabara, N., Shimizu, N., Kravukhina, E., Uchiyama, S., Fukamizu, A., and Shimizu, T. (2016) Novel helical assembly in arginine methyltransferase 8. *J. Mol. Biol.* **428**, 1197–1208
39. Willert, E. K., and Phillips, M. A. (2009) Cross-species activation of trypanosome S-adenosylmethionine decarboxylase by the regulatory subunit prozyme. *Mol. Biochem. Parasitol.* **168**, 1–6
40. Pils, B., and Schultz, J. (2004) Inactive enzyme-homologues find new function in regulatory processes. *J. Mol. Biol.* **340**, 399–404
41. Adrain, C., and Freeman, M. (2012) New lives for old: evolution of pseudoenzyme function illustrated by iRhoms. *Nat. Rev. Mol. Cell Biol.* **13**, 489–498
42. Ivanov, I. P., Firth, A. E., and Atkins, J. F. (2010) Recurrent emergence of catalytically inactive ornithine decarboxylase homologous forms that likely have regulatory function. *J. Mol. Evol.* **70**, 289–302
43. Nguyen, S., Leija, C., Kinch, L., Regmi, S., Li, Q., Grishin, N. V., and Phillips, M. A. (2015) Deoxyhypusine modification of eukaryotic translation initiation factor 5A (eIF5A) is essential for *Trypanosoma brucei* growth and for expression of polyprolyl-containing proteins. *J. Biol. Chem.* **290**, 19987–19998
44. Xiao, Y., Nguyen, S., Kim, S. H., Volkov, O. A., Tu, B. P., and Phillips, M. A. (2013) Product feedback regulation implicated in translational control of the *Trypanosoma brucei* S-adenosylmethionine decarboxylase regulatory subunit prozyme. *Mol. Microbiol.* **88**, 846–861
45. Nett, I. R., Martin, D. M., Miranda-Saavedra, D., Lamont, D., Barber, J. D., Mehler, A., and Ferguson, M. A. (2009) The phosphoproteome of bloodstream form *Trypanosoma brucei*, causative agent of African sleeping sickness. *Mol. Cell. Proteomics* **8**, 1527–1538
46. Lueong, S., Merce, C., Fischer, B., Hoheisel, J. D., and Erben, E. D. (2016) Gene expression regulatory networks in *Trypanosoma brucei*: insights into the role of the mRNA-binding proteome. *Mol. Microbiol.* **100**, 457–471
47. Fritz, M., Vanselow, J., Sauer, N., Lamer, S., Goos, C., Siegel, T. N., Subota, I., Schlosser, A., Carrington, M., and Kramer, S. (2015) Novel insights into RNP granules by employing the trypanosome's microtubule skeleton as a molecular sieve. *Nucleic Acids Res.* **43**, 8013–8032
48. Wang, P., Doxtader, K. A., and Nam, Y. (2016) Structural basis for cooperative function of Mettl3 and Mettl14 methyltransferases. *Mol. Cell* **63**, 306–317
49. Wang, X., Feng, J., Xue, Y., Guan, Z., Zhang, D., Liu, Z., Gong, Z., Wang, Q., Huang, J., Tang, C., Zou, T., and Yin, P. (2016) Structural basis of N⁶-adenosine methylation by the METTL3-METTL14 complex. *Nature* **534**, 575–578
50. Liu, J., Yue, Y., Han, D., Wang, X., Fu, Y., Zhang, L., Jia, G., Yu, M., Lu, Z., Deng, X., Dai, Q., Chen, W., and He, C. (2014) A METTL3-METTL14

T. brucei PRMTs are an Enzyme-Prozyme Pair

- complex mediates mammalian nuclear RNA N⁶-adenosine methylation. *Nat. Chem. Biol.* **10**, 93–95
51. Iyer, L. M., Zhang, D., and Aravind, L. (2016) Adenine methylation in eukaryotes: apprehending the complex evolutionary history and functional potential of an epigenetic modification. *Bioessays* **38**, 27–40
52. Miranda, T. B., Miranda, M., Frankel, A., and Clarke, S. (2004) PRMT7 is a member of the protein arginine methyltransferase family with a distinct substrate specificity. *J. Biol. Chem.* **279**, 22902–22907
53. Hasegawa, M., Toma-Fukai, S., Kim, J. D., Fukamizu, A., and Shimizu, T. (2014) Protein arginine methyltransferase 7 has a novel homodimer-like structure formed by tandem repeats. *FEBS Lett.* **588**, 1942–1948
54. Hadjikyriacou, A., Yang, Y., Espejo, A., Bedford, M. T., and Clarke, S. G. (2015) Unique features of human protein arginine methyltransferase 9 (PRMT9) and its substrate RNA splicing factor SF3B2. *J. Biol. Chem.* **290**, 16723–16743
55. Yang, Y., Hadjikyriacou, A., Xia, Z., Gayatri, S., Kim, D., Zurita-Lopez, C., Kelly, R., Guo, A., Li, W., Clarke, S. G., and Bedford, M. T. (2015) PRMT9 is a type II methyltransferase that methylates the splicing factor SAP145. *Nat. Commun.* **6**, 6428
56. Weiss, V. H., McBride, A. E., Soriano, M. A., Filman, D. J., Silver, P. A., and Hogle, J. M. (2000) The structure and oligomerization of the yeast arginine methyltransferase, Hmt1. *Nat. Struct. Biol.* **7**, 1165–1171
57. Wang, C., Zhu, Y., Chen, J., Li, X., Peng, J., Chen, J., Zou, Y., Zhang, Z., Jin, H., Yang, P., Wu, J., Niu, L., Gong, Q., Teng, M., and Shi, Y. (2014) Crystal structure of arginine methyltransferase 6 from *Trypanosoma brucei*. *PLoS One* **9**, e87267
58. Herrmann, F., Pably, P., Eckerich, C., Bedford, M. T., and Fackelmayer, F. O. (2009) Human protein arginine methyltransferases *in vivo*—distinct properties of eight canonical members of the PRMT family. *J. Cell Sci.* **122**, 667–677
59. Lim, Y., Kwon, Y. H., Won, N. H., Min, B. H., Park, I. S., Paik, W. K., and Kim, S. (2005) Multimerization of expressed protein-arginine methyltransferases during the growth and differentiation of rat liver. *Biochim. Biophys. Acta* **1723**, 240–247
60. Pak, M. L., Lakowski, T. M., Thomas, D., Vhuyian, M. I., Hüsecken, K., and Frankel, A. (2011) A protein arginine N-methyltransferase 1 (PRMT1) and 2 heteromeric interaction increases PRMT1 enzymatic activity. *Biochemistry* **50**, 8226–8240
61. Weimann, M., Grossmann, A., Woodsmith, J., Özkan, Z., Birth, P., Meierhofer, D., Benlasfer, N., Valovka, T., Timmermann, B., Wanker, E. E., Sauer, S., and Stelzl, U. (2013) A Y2H-seq approach defines the human protein methyltransferase interactome. *Nat. Methods* **10**, 339–342
62. Huttlin, E. L., Ting, L., Bruckner, R. J., Gebreb, F., Gygi, M. P., Szpyt, J., Tam, S., Zarraga, G., Colby, G., Baltier, K., Dong, R., Guarani, V., Vaite, L. P., Ordureau, A., Rad, R., *et al.* (2015) The BioPlex Network: a systematic exploration of the human interactome. *Cell* **162**, 425–440
63. Lee, J., Sayegh, J., Daniel, J., Clarke, S., and Bedford, M. T. (2005) PRMT8, a new membrane-bound tissue-specific member of the protein arginine methyltransferase family. *J. Biol. Chem.* **280**, 32890–32896
64. Rolland, T., Taşan, M., Charlotheaux, B., Pevzner, S. J., Zhong, Q., Sahni, N., Yi, S., Lemmens, I., Fontanillo, C., Mosca, R., Kamburov, A., Ghiassian, S. D., Yang, X., Ghamsari, L., Balcha, D., *et al.* (2014) A proteome-scale map of the human interactome network. *Cell* **159**, 1212–1226
65. Niu, L., Zhang, Y., Pei, Y., Liu, C., and Cao, X. (2008) Redundant requirement for a pair of PROTEIN ARGININE METHYLTRANSFERASE4 homologs for the proper regulation of *Arabidopsis* flowering time. *Plant Physiol.* **148**, 490–503
66. Wirtz, E., Leal, S., Ochatt, C., and Cross, G. A. (1999) A tightly regulated inducible expression system for conditional gene knock-outs and dominant-negative genetics in *Trypanosoma brucei*. *Mol. Biochem. Parasitol.* **99**, 89–101
67. Baltz, T., Baltz, D., Giroud, C., and Crockett, J. (1985) Cultivation in a semi-defined medium of animal infective forms of *Trypanosoma brucei*, *T. equiperdum*, *T. evansi*, *T. rhodesiense* and *T. gambiense*. *EMBO J.* **4**, 1273–1277
68. Morriswood, B., Havlicek, K., Demmel, L., Yavuz, S., Sealey-Cardona, M., Vidilaseris, K., Anrather, D., Kostan, J., Djinovic-Carugo, K., Roux, K. J., and Warren, G. (2013) Novel bilobe components in *Trypanosoma brucei* identified using proximity-dependent biotinylation. *Eukaryot. Cell* **12**, 356–367
69. Hayman, M. L., Miller, M. M., Chandler, D. M., Goulah, C. C., and Read, L. K. (2001) The trypanosome homolog of human p32 interacts with RBP16 and stimulates its gRNA binding activity. *Nucleic Acids Res.* **29**, 5216–5225
70. Pelletier, M., Xu, Y., Wang, X., Zahariev, S., Pongor, S., Aletta, J. M., and Read, L. K. (2001) Arginine methylation of a mitochondrial guide RNA binding protein from *Trypanosoma brucei*. *Mol. Biochem. Parasitol.* **118**, 49–59

The Major Protein Arginine Methyltransferase in *Trypanosoma brucei* Functions as an Enzyme-Prozyme Complex

Lucie Kafková, Erik W. Debler, John C. Fisk, Kanishk Jain, Steven G. Clarke and Laurie K. Read

J. Biol. Chem. 2017, 292:2089-2100.

doi: 10.1074/jbc.M116.757112 originally published online December 20, 2016

Access the most updated version of this article at doi: [10.1074/jbc.M116.757112](https://doi.org/10.1074/jbc.M116.757112)

Alerts:

- [When this article is cited](#)
- [When a correction for this article is posted](#)

[Click here](#) to choose from all of JBC's e-mail alerts

This article cites 70 references, 34 of which can be accessed free at <http://www.jbc.org/content/292/6/2089.full.html#ref-list-1>